

## Article

# Cannabidiol Mediates Beneficial Effects on the Microvasculature of Murine Hearts with Regard to Irradiation-Induced Inflammation and Early Signs of Fibrosis

Lisa Bauer <sup>1,2</sup>, Bayan Alkotub <sup>3,4</sup>, Markus Ballmann <sup>5</sup>, Khoulood Hachani <sup>6</sup>, Mengyao Jin <sup>5</sup>, Morteza Hasanzadeh Kafshgari <sup>2</sup>, Gerhard Rammes <sup>5</sup>, Alan Graham Pockley <sup>7</sup> and Gabriele Multhoff <sup>1,2,\*</sup>

<sup>1</sup> Department of Radiation Oncology, TUM School of Medicine and Health, University Hospital of the Technical University of Munich (TUM), 81675 Munich, Germany; lisa.bauer@tum.de

<sup>2</sup> Radiation Immuno-Oncology Group, Central Institute for Translational Cancer Research (TranslaTUM), TUM School of Medicine and Health, University Hospital of the Technical University of Munich (TUM), Einstein Str. 25, 81675 Munich, Germany; morteza.kafshgari@tum.de

<sup>3</sup> Institute of Biological and Medical Imaging, Bioengineering Center, Helmholtz Zentrum München, 85764 Neuherberg, Germany; bayan.alkotub@tum.de

<sup>4</sup> Biological Imaging, Central Institute for Translational Cancer Research (TranslaTUM), TUM School of Medicine and Health & TUM School of Computation, Information and Technology, Technical University of Munich, 81675 Munich, Germany

<sup>5</sup> Department of Anaesthesiology and Intensive Care Medicine, TUM School of Medicine and Health, University Hospital of the Technical University of Munich (TUM), 81675 Munich, Germany; markus.ballmann@tum.de (M.B.); mengyao.jin@tum.de (M.J.); g.rammes@tum.de (G.R.)

<sup>6</sup> Department of Otolaryngology, Head and Neck Surgery, TUM School of Medicine and Health, University Hospital of the Technical University of Munich (TUM), 81675 Munich, Germany; khoulood.hachani@tum.de

<sup>7</sup> John van Geest Cancer Research Centre, School of Science and Technology, Nottingham Trent University, Nottingham NG11 8NS, UK; graham.pockley@ntu.ac.uk

\* Correspondence: gabriele.multhoff@tum.de; Tel.: +49-89-4140-4514; Fax: +49-89-4140-4299

**Simple Summary:** Radiotherapy of thoracic malignancies, such as lung or breast cancer, involves exposure of the heart to relevant mean radiation doses that are associated with an increased risk of developing cardiovascular disease and mediated by chronic vessel inflammation. In this study, we investigated whether cannabidiol (CBD), the non-psychogenic component of cannabis, can prevent irradiation-induced vessel inflammation and consequently protect mice from the development of heart diseases. We demonstrated that a continuous treatment of mice with CBD starting before irradiation attenuates endothelial cell inflammation, immune infiltration, and onset of cardiac fibrosis. Therefore, CBD is a promising candidate to alleviate the risk of irradiation-induced heart disease.

**Abstract:** Objective: Radiotherapy administered to control thoracic cancers results in a partial irradiation of the heart at mean doses up to 19 Gy, which increases the risk of developing a spectrum of cardiovascular diseases known as radiation-induced heart disease (RIHD). As inflammation is a major driver of the development of RIHD, we investigated the potential of the anti-inflammatory agent cannabidiol (CBD) to attenuate irradiation-induced cardiovascular damage in vivo. Methods: Female C57BL/6 mice were given daily injections of CBD (i.p., 20 mg/kg body weight) for 4 weeks beginning either 2 weeks prior to 16 Gy irradiation of the heart or at the time of irradiation. Mice were sacrificed 30 min and 2, 4, and 10 weeks after irradiation to investigate the expression of inflammatory markers and stress proteins in primary cardiac endothelial cells (ECs). DNA double-strand breaks, immune cell infiltration, and signs of fibrosis were studied in explanted heart tissue. Results: We showed that the irradiation-induced upregulation of the inflammatory markers ICAM-1 and MCAM was only attenuated when treatment with CBD was started 2 weeks prior to irradiation but not when the CBD treatment was started concomitant with



Academic Editor: Jason Parsons

Received: 26 March 2025

Revised: 22 April 2025

Accepted: 19 May 2025

Published: 21 May 2025

**Citation:** Bauer, L.; Alkotub, B.; Ballmann, M.; Hachani, K.; Jin, M.; Hasanzadeh Kafshgari, M.; Rammes, G.; Pockley, A.G.; Multhoff, G. Cannabidiol Mediates Beneficial Effects on the Microvasculature of Murine Hearts with Regard to Irradiation-Induced Inflammation and Early Signs of Fibrosis. *Radiation* **2025**, *5*, 17. <https://doi.org/10.3390/radiation5020017>

**Copyright:** © 2025 by the authors. Licensee MDPI, Basel, Switzerland. This article is an open access article distributed under the terms and conditions of the Creative Commons Attribution (CC BY) license (<https://creativecommons.org/licenses/by/4.0/>).

irradiation of the heart. The protective effect of CBD was associated with a decrease in irradiation-induced DNA damage and an increased expression of protective heat shock proteins (Hsp), such as Hsp32/Heme-oxygenase-1 (HO-1) and Hsp70, in the heart tissue. While the upregulation of the inflammatory markers ICAM-1 and MCAM, expression was prevented up to 10 weeks after irradiation by CBD pre-treatment, and the expression of VCAM-1, which started to increase 10 weeks after irradiation, was further upregulated in CBD pre-treated mice. Despite this finding, 10 weeks after heart irradiation, immune cell infiltration and fibrosis markers of the heart were significantly reduced in CBD pre-treated mice. Conclusion: CBD treatment before irradiation mediates beneficial effects on murine hearts of mice, resulting in a reduction of radiation-induced complications, such as vascular inflammation, immune cell infiltration, and fibrosis.

**Keywords:** radiotherapy; cannabidiol (CBD); irradiation-induced heart disease; vascular inflammation; fibrosis

## 1. Introduction

Radiotherapy is an indispensable part of cancer therapy for more than 50% of patients with solid tumors [1,2]. However, the beneficial anti-tumor effects of ionizing irradiation are hampered by toxicity to normal, non-cancerous tissue surrounding the tumor [3], which can result in radiation-induced lung (RILD) [4] and liver diseases [5]. Due to the fact that cardiac cells are non-proliferative, the heart has been considered a radioresistant organ. However, epidemiological studies have indicated that patients receiving radiotherapy for the local control of thoracic malignancies had a higher incidence of developing cardiovascular diseases years and decades after radiotherapy [6,7]. Despite careful irradiation dose treatment planning for patients with left-sided thoracic cancers, the mean dose rate to the heart ranges between 3.6 and 4.6 Gy, with maximum doses up to 19 Gy [8,9].

Radiotherapy-induced heart failure is mainly mediated by chronic inflammation, which is induced by multiple microlesions in endothelial cells (ECs) and cardiomyocytes, which drive a continuous release of inflammatory signals [3,10]. In chronic inflammation, the wound healing response persists because the body's immune system is unable to resolve the damage [11,12]. Functionally, persisting inflammation is characterized by an ongoing upregulation in the expression of cellular adhesion molecules (CAMs) on ECs. This results in increased attachment and infiltration of immune cells into the vessel wall [3], which supports the formation of plaques and thickening of the vascular wall, a process termed atherosclerosis. Over time, decreased blood flow causes a subsequent undersupply of the affected heart tissue with oxygen and nutrients [6]. Eventually, a completely closed vessel may cause heart infarction, or a ruptured plaque of the heart may induce vessel occlusion in other tissues, such as the brain, resulting in a stroke [6]. Another complication of a persistent wound healing response is cardiac fibrosis [6,13]. An excess deposition of extracellular matrix components in the heart, which causes stiffening of the cardiac muscle or the heart valves, results in cardiomyopathy or valvular heart disease [6].

Due to the central role of inflammation in the development of radiation-induced heart diseases (RIDHs), which generally develop in human patients a decade after radiotherapy [14], anti-inflammatory agents could provide a useful preventative approach to reduce the risk for RIDH. The pathophysiology of RIDH is characterized by major functional changes in the microvasculature of the myocardium [15]. However, because the anti-cancer efficacy of radiotherapy relies on an active immune system [16], an anti-inflammatory drug improving normal tissue toxicity of radiotherapy may impair protective anti-tumor immune responses. CBD has been shown to mediate anti-oxidative and anti-inflammatory

effects in a variety of cell types and inflammatory disease models [17] while simultaneously showing pro-apoptotic, anti-angiogenic, and anti-metastatic activity in a variety of cancer models [18]. Moreover, CBD has shown promising results in attenuating cardiac dysfunctions [19], and it has a favorable safety profile in clinical use [20].

Therefore, we hypothesize that CBD mediates protective effects on irradiation-induced cardiac damage while preserving anti-tumor activity. In this study, we investigated the effects of different CBD treatment schedules on radiation-induced vessel inflammation, immune infiltration, DNA damage, and early fibrosis in C57BL/6 mice receiving a single irradiation dose of 16 Gy to 80% of the heart, a clinically relevant mean heart dose after radiotherapy of patients with thoracic malignancies [8,9].

## 2. Materials and Methods

**Animals, CBD treatment, and irradiation:** Animal experiments were performed in accordance with the German Animal Welfare Act (TierSchutzGesetz). All animal experiments were performed in compliance with the institutional guidelines of the University Hospital of the Technical University of Munich and approved by the Regierung von Oberbayern (licence ROB-55.2-2532.Vet\_02-21-195 and ROB-55.2-2532.Vet\_02-23-53). Mice were housed under sterile conditions (food and water ad libitum,  $23 \pm 0.5$  °C, 12 h light/dark cycle).

Female 10-week-old C57BL/6 mice (Charles River, Sulzfeld, Germany) were divided into 4 treatment groups. Group 1 (control) received a 0 Gy sham irradiation, and group 2 received a local image-guided single dose of partial irradiation (16 Gy) of the heart (80%) with minor exposure to the lung (20%) using the Small Animal Radiation Research Platform (SARRP, X-Strahl, Walsall Wood, UK) and the software SARRP Control and Muriplan [21]. Irradiation was performed using 220 kV and 13 mA X-ray beams filtered with copper (0.15 mm) under cone beam computed tomography (CBCT) guidance. In each of the 3 CT scan projections (transverse, sagittal, and frontal), the hearts and lungs of the mice were marked. The planning system was carried out with a calibrated ionization chamber (International Atomic Energy Agency, Vienna, Austria) and radiochromic Gafchromic films (EBT3, Ashland, Covington, KY, USA). Group 3 received the same irradiation treatment combined with daily injections (i.p.) of CBD (Phytolab, Vestenbergsgreuth, Germany) at a concentration of 20 mg/kg body weight [19] dissolved in saline (B. Braun Melsungen, Melsungen, Germany), Tween 20 (Sigma-Aldrich, Taufkirchen, Germany), and DMSO (Sigma-Aldrich) at a ratio of 18:1:1 for 4 weeks. Group 4 received daily CBD injections with 0 Gy sham irradiation for 4 weeks. Treatments were scheduled as follows: mice received partial heart (80%) and lung (20%) irradiation (16 Gy) on day 1 with simultaneous onset of daily i.p. injections of CBD (20 mg/kg body weight) lasting for 4 weeks, and mice received daily i.p. injections of CBD 2 weeks before irradiation (16 Gy), which continued for another 2 weeks after partial irradiation of the heart (80%) and lung (20%). Mice were sacrificed through cervical dislocation 30 min and 2, 4, and 10 weeks post-irradiation. All procedures were performed under isoflurane anesthesia (CP Pharma, Burgdorf, Germany). The number of mice used for each experiment is indicated in the legend of each figure.

**Heart digestion:** Heart tissue was minced and then digested in collagenase A (Roche, Penzberg, Germany) (0.002 g/mL in HBSS (Gibco ThermoFisher Scientific, Darmstadt, Germany, Sigma-Aldrich) +10% *v/v* fetal bovine serum (FBS, Sigma-Aldrich) for 45 min under rotation. The pre-digested tissue was further dissociated by aspirating it 10 times through an 18 G needle, followed by filtration through a 70  $\mu$ m mesh and two rounds of washing in HBSS/10% *v/v* FBS. The resulting single cell suspensions were used for flow cytometry analysis and Western blotting.

**Flow cytometry:** After washing the cells with Dulbecco's PBS (DPBS) supplemented with 10% *v/v* FBS ('flow cytometry buffer'), they were incubated with the following

fluorescence-labeled monoclonal antibodies (mAbs; Table 1) for 30 min at 4 °C in the dark. After another washing step, cells were resuspended in flow cytometry buffer containing propidium iodide (PI). Data were acquired on a MACSQuant<sup>®</sup> flow cytometer (Miltenyi Biotec, Bergisch Gladbach, Germany) and analyzed using FlowJo<sup>™</sup> software V10.10 (BD Biosciences, Franklin Lakes, NJ, USA). Live cells (PI-negative) and cardiac ECs (CD31<sup>+</sup>/CD45<sup>-</sup>) or leukocytes (CD31<sup>-</sup>/CD45<sup>+</sup>) were gated with the indicated markers, and the percentage of positively stained cells and the median signal intensity (MFI) were determined in each experiment.

**Table 1.** Fluorescence-labeled antibodies for flow cytometry.

Antibody (Clone)	Dilution	Company
CD31-APC (MEC 13.3)	1:4	BD Biosciences
CD34-FITC (RAM34)	1:10	eBioscience (ThermoFisher Scientific)
CD45-Vio Blue (REA737)	1:10	Miltenyi Biotec
CD54 (ICAM-1)-FITC (3E2)	no	BD Biosciences
CD61 (Integrin $\beta$ -3)-FITC (HM $\beta$ 3-1)	no	BD Biosciences
CD102 (ICAM-2)-FITC (3C4 mIC2/4)	1:10	BD Biosciences
CD105 (Endoglin)-PE MJ7/18)	1:4	eBioscience (ThermoFisher Scientific)
CD106 (VCAM-1)-PE (M/K-2)	1:2	Invitrogen (ThermoFisher Scientific)
CD144 (VE-cadherin)-PE (11D4.1)	1:4	BD Biosciences
CD146 (MCAM)-PE (ME-9F1)	1:4	BD Biosciences

**Western blotting:** Heart tissue was lysed in radioimmunoprecipitation assay (RIPA) buffer containing protease cocktail tablets (cOmplete tablets, Roche Diagnostic GmbH, Basel, Switzerland) and phosphatase inhibitors (PhosphoSTOP, Roche Diagnostic GmbH). The protein concentration was determined using the Pierce<sup>™</sup> BCA Protein Assay Kit (ThermoFisher Scientific, Waltham, MA, USA), and 20  $\mu$ g of protein lysate was separated on an SDS-PAGE (8–15% *v/v*) gel. After transfer onto activated polyvinylidene fluoride membranes (PVDFs) and blocking in 1 $\times$  Roti block buffer for 1 h at room temperature (RT), membranes were incubated with primary antibodies (Table 2) diluted in 1 $\times$  Roti block buffer at 4 °C overnight under rotation. After another washing step, membranes were stained with the relevant secondary HRP-conjugated antibodies (Dako-Agilent, Santa Clara, CA, USA; BD Biosciences, Franklin Lakes, NJ, USA; Table 2) diluted in 1 $\times$  Roti block buffer for 60 min at RT. The Pierce<sup>™</sup> ECL Western Kit (ThermoFisher Scientific) was used to visualize the protein bands, and images were acquired using the ChemiDoc<sup>™</sup> Touch Imaging System (Bio-Rad, Hercules, CA, USA). The protein expression ratio for each sample was quantified using ImageJ 6.1 Software. If not indicated otherwise, the dilution of the antibodies was 1:1000.

**Table 2.** Antibodies for Western blot analysis.

Antibody (Dilution)	Company
$\beta$ -Actin (1:10,000)	Sigma-Aldrich
CD14	Invitrogen
Col3a1	Santa Cruz Biotechnology
Decorin	Abcam
Fibronectin	Invitrogen
Heme-oxygenase-1 (HO-1)	Cell Signaling Technology
Hsp70	multimmune GmbH
$\gamma$ -H2AX (1:5000)	Abcam
HRP-conjugated rabbit anti-mouse Ig (1:2000)	Dako-Agilent
HRP-conjugated swine anti-rabbit Ig	BD Biosciences

**Statistical analysis:** Statistical analyses were performed using GraphPad Prism 10 V10.0.2 (GraphPad Software, Boston, MA, USA), and data are presented as mean ± standard deviation (SD) of at least three independent experiments. Differences between groups were assessed using either one-way ANOVA followed by Tukey’s post hoc test (multiple comparisons) or two-way ANOVA followed by Tukey’s multiple comparisons test (experiments involving more than 2 conditions). Statistical significance was defined as a *p* value of less than 0.05. Significance levels are defined as \* *p* < 0.05, \*\* *p* < 0.01, \*\*\* *p* < 0.001, and \*\*\*\* *p* < 0.0001.

### 3. Results

#### CBD treatment starting simultaneous with irradiation does not reduce the expression of inflammatory markers on heart ECs

Chronic inflammation in cardiac tissue induced by irradiation is characterized by an upregulated expression of CAMs on ECs [10,22], which participate in the adhesion and transmigration of leukocytes in damaged tissue [23–25]. Therefore, this study measured the expression of MCAM, ICAM-1, ICAM-2, and VCAM-1 on primary heart ECs of mice (n = 4) 4 weeks after receiving sham irradiation in vivo (0 Gy, group 1), partial heart (80%) and lung (20%) irradiation (16 Gy, group 2), and a combination of daily i.p. CBD (20 mg/kg body weight) treatment starting on day 1 simultaneous with irradiation (16 Gy) and continuing for 4 weeks (group 3) (Figure 1, treatment schedule).

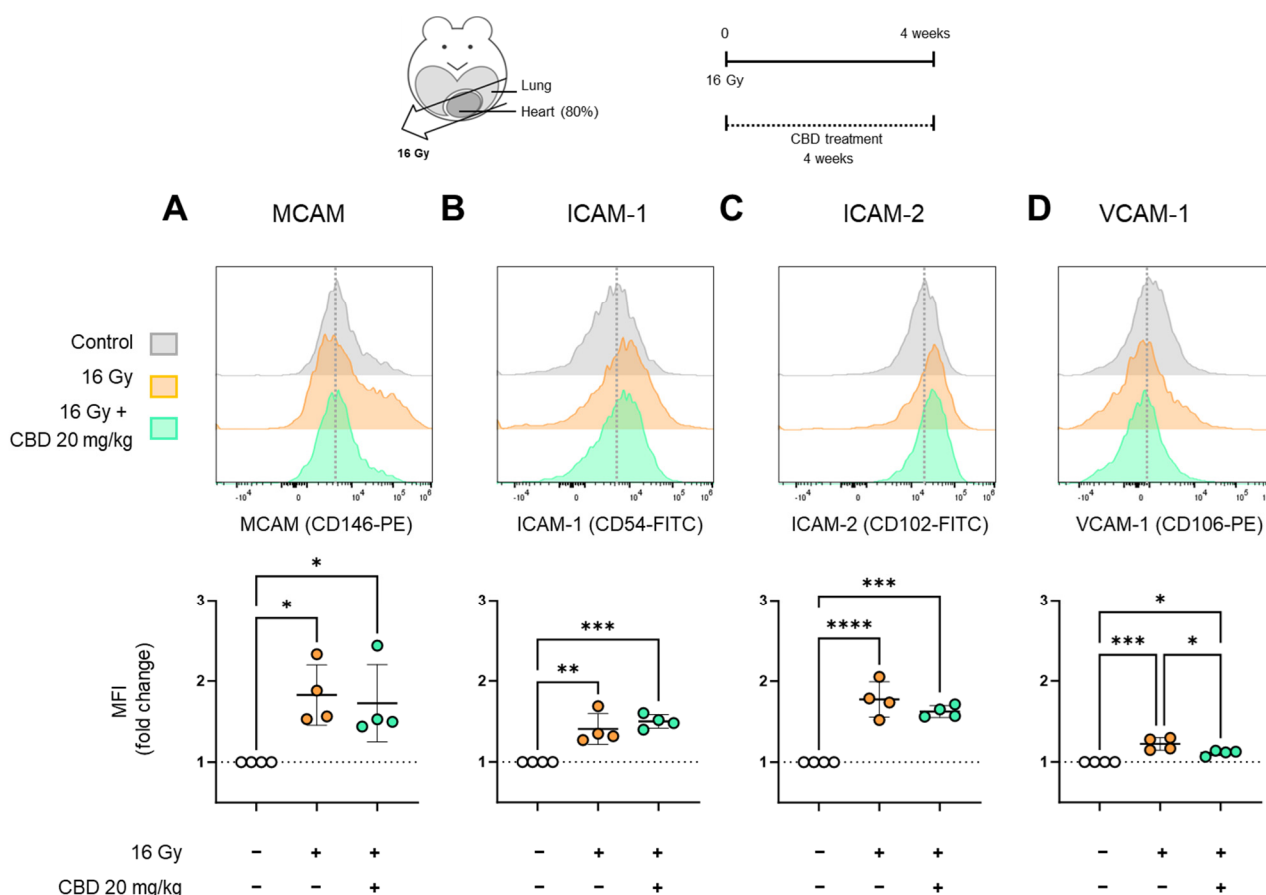


**Figure 1.** Representative fluorescence histograms of (A) MCAM, (B) ICAM-1, (C) ICAM-2, and (D) VCAM-1 expression and median signal intensity (MFI) on primary cardiac ECs (CD31<sup>+</sup>/CD45<sup>-</sup>) of C57BL/6 mice 4 weeks after receiving 0 Gy sham irradiation (white), 16 Gy irradiation (orange), or 16 Gy irradiation with daily CBD treatment starting after irradiation (i.p., 20 mg/kg body weight for 4 weeks; green); data represent mean values ± SD of 4 mice (n = 4); \* *p* < 0.05, \*\* *p* < 0.01, \*\*\* *p* < 0.001, and \*\*\*\* *p* < 0.0001.

Single cell suspensions were prepared from freshly resected hearts of mice of the different groups after 4 weeks, and the median signal intensity (MFI) of expression of MCAM (Figure 1A), ICAM-1 (Figure 1B), ICAM-2 (Figure 1C), and VCAM-1 (Figure 1D) on CD31<sup>+</sup>/CD45<sup>-</sup> gated ECs was assessed through multicolor flow cytometry. The gating strategy of expression of MCAM, as an example, is illustrated in Appendix A.1.

The expression density of MCAM on primary heart ECs showed a significant increase 4 weeks after irradiation compared to sham-irradiated control mice, and continuous CBD treatment (4 weeks) starting on the day of partial heart/lung irradiation (16 Gy) did not significantly alter the upregulated expression of MCAM (Figure 1A). The same expression pattern is observed for other inflammatory markers, such as ICAM-1 (Figure 1B) and ICAM-2 (Figure 1C). With respect to the expression density of VCAM-1, irradiation-induced upregulation on heart ECs was lower compared to the other inflammatory markers and compared to sham-irradiated controls, and it was significantly reduced by 4-week continuous CBD treatment (Figure 1D). This indicates that CBD treatment that starts on the day of irradiation reduces the elevated expression of VCAM-1 but not that of MCAM, ICAM-1, or ICAM-2.

#### **CBD treatment starting 2 weeks before irradiation reduced the expression of inflammatory markers on heart ECs**

Because the anti-inflammatory effects of CBD are associated with antioxidant pathways [26,27] and an upregulated expression of the stress protein Hsp32/HO-1 [28], the CBD pre-treatment was started 2 weeks before and continued for another 2 weeks after irradiation to allow for the synthesis of protective anti-oxidative proteins (Figure 2, treatment schedule). Mice receiving sham irradiation (0 Gy), partial irradiation of the heart (80%) and lung (20%) with 16 Gy, or a combined treatment of daily i.p. injections of CBD (20 mg/kg body weight, 4 weeks) beginning 2 weeks prior and continuing another 2 weeks after irradiation (16 Gy) were sacrificed 2 weeks (n = 5) or 10 weeks after irradiation (n = 3–4) (Figure 2), and the hearts were resected to measure the expression density of the inflammatory markers MCAM (Figure 2A), ICAM-1 (Figure 2B), and ICAM-2 (Figure 2C) on CD31<sup>+</sup>/CD45<sup>-</sup> ECs.

The MFI of the MCAM expression was significantly increased on cardiac ECs 2 weeks and, even more pronounced, 10 weeks after partial heart irradiation compared to the control group (Figure 2A). Daily CBD treatment of mice beginning two weeks prior to irradiation and lasting another 2 weeks after irradiation resulted in a reduction of MCAM expression, which reached a statistically significant difference after 10 weeks (Figure 2A). Similarly, the expression densities of ICAM-1 (Figure 2B) and ICAM-2 (Figure 2C), which were significantly increased 2 weeks and even more pronounced 10 weeks after irradiation, were decreased in mice receiving CBD treatment 2 weeks prior to irradiation. A significant decrease in the expression density of ICAM-1 was detected at 10 weeks compared to irradiated mice (Figure 2B). This attenuating effect of CBD on the irradiation-induced upregulation of MCAM, ICAM-1, and ICAM-2 expression 2 and 10 weeks after irradiation was only observed when CBD was administered for 2 weeks before and continued for another 2 weeks after irradiation but not when the 4-week CBD treatment was started concomitant with irradiation. These findings indicate that CBD protects heart ECs against radiation-induced damage rather than repairing radiation-induced damage. Because the attenuating effect on the expression of inflammatory markers persists for at least 10 weeks after irradiation, despite the fact that CBD treatment was terminated 2 weeks after irradiation, we hypothesize that CBD treatment protects against acute and also chronic radiation-induced damage of heart ECs.

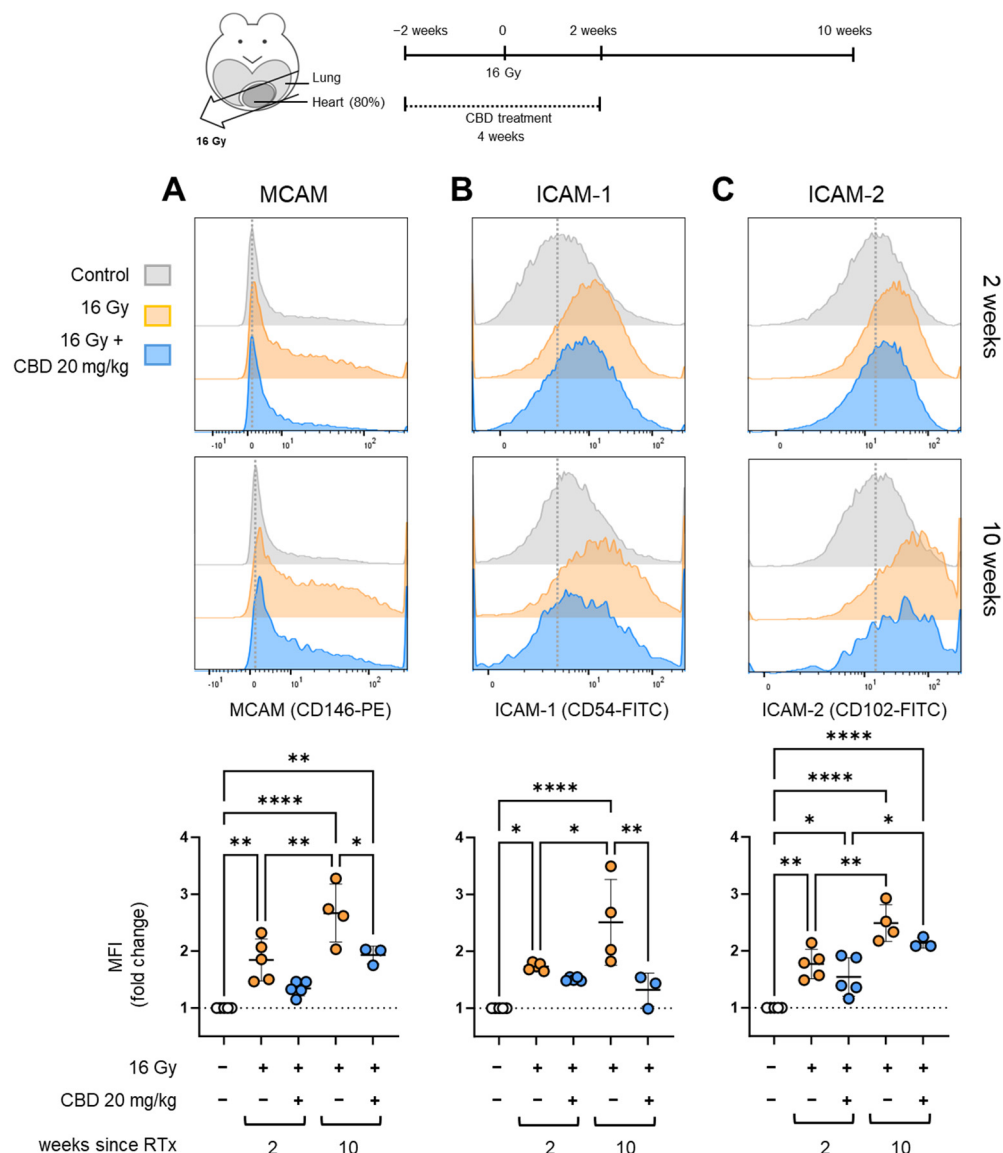


**Figure 2.** Representative fluorescence histograms of (A) MCAM, (B) ICAM-1, and (C) ICAM-2 expression and median signal intensity (MFI) on primary cardiac ECs (CD31<sup>+</sup>/CD45<sup>-</sup>) of C57BL/6 mice 2 (n = 5) and 10 weeks (n = 3–4) after receiving 0 Gy sham irradiation (white), 16 Gy irradiation (orange), or 16 Gy irradiation with daily CBD treatment starting 2 weeks prior to irradiation (i.p., 20 mg/kg body weight for 4 weeks; blue); data represent mean values ± SD of 3–5 mice (n = 3–5); \* *p* < 0.05, \*\* *p* < 0.01 and \*\*\*\* *p* < 0.0001.

### The anti-inflammatory effect of CBD treatment starting 2 weeks before irradiation is associated with increased stress protein synthesis in heart ECs

To investigate the role of stress proteins in the attenuation of irradiation-induced damage in heart ECs, levels of Hsp32/HO-1 and Hsp70 were measured in whole heart lysates of mice (n = 3–4) receiving either sham irradiation (0 Gy), partial heart (80%) and lung (20%) irradiation with 16 Gy, or irradiation of the heart (16 Gy) combined with daily i.p. injections of CBD (20 mg/kg body weight) for 4 weeks, beginning 2 weeks prior to and lasting 2 weeks after irradiation (Figure 3, treatment scheme). All mice were sacrificed two weeks after partial heart/lung irradiation. Neither Hsp32/HO-1 (Figure 3A) nor Hsp70 levels were altered significantly in heart lysates of mice two weeks after irradiation with 16 Gy. CBD treatment alone also did not change the levels of Hsp70 in mouse heart cells. However, CBD treatment of mice 2 weeks before and 2 weeks after irradiation led

to a significant upregulation of Hsp32/HO-1 and Hsp70 levels in heart cells 2 weeks after irradiation (Figure 3A, B). Elevated levels of Hsp32/HO-1 and Hsp70 have been shown to adapt cells to oxidative stress [29] and may therefore contribute to the attenuated expression of the inflammatory markers after irradiation.

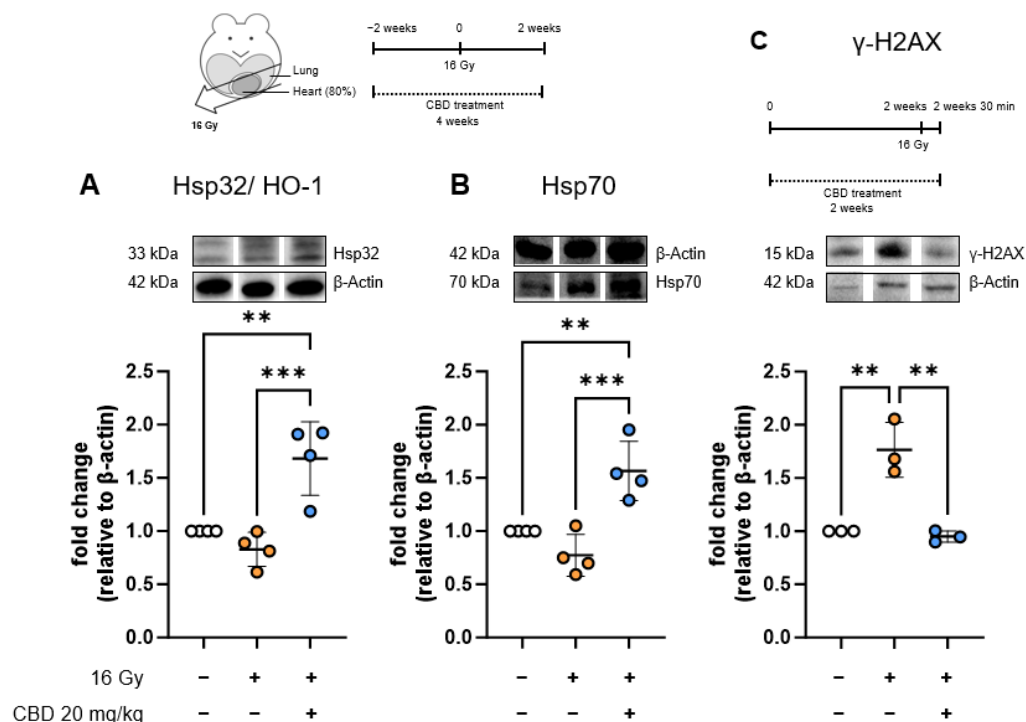


**Figure 3.** Representative Western blots (images spliced from the same blot) and mean protein levels relative to β-actin of (A) Hsp32/HO-1 (n = 4) and (B) Hsp70 (n = 4) of whole heart lysate of C57BL/6 mice 2 weeks after receiving 0 Gy sham irradiation (left lane, white symbol), 16 Gy irradiation (center lane, orange symbol), or 16 Gy irradiation with daily CBD treatment starting 2 weeks prior to irradiation (i.p., 20 mg/kg body weight for 4 weeks; right lane, blue symbol); (C) representative Western blot and mean γ-H2AX protein levels (n = 3) relative to control of whole heart lysate of C57BL/6 mice 30 min after receiving 0 Gy sham irradiation (left lane, white symbol), 16 Gy irradiation (center lane, orange symbol), or 16 Gy irradiation with daily CBD treatment starting 2 weeks prior to irradiation (i.p., 20 mg/kg body weight; right lane, blue symbol); data represent mean values ± SD of 3–4 mice (n = 3–4); \*\* *p* < 0.01, \*\*\* *p* < 0.001.

As an indicator of irradiation-induced stress, the occurrence of DNA double-strand breaks was detected based on γ-H2AX expression in whole heart lysates of mice (n = 3) that received sham irradiation (0 Gy), irradiation of the heart (80%) and lung (20%) with 16 Gy, or partial heart irradiation (16 Gy) combined with daily i.p. injections of CBD (20 mg/kg body weight) for 4 weeks beginning 2 weeks prior to irradiation and lasting for another 2 weeks. The histone γ-H2AX responds rapidly to DNA double-strand breaks and can only be detected within a short time window after irradiation [30]. Therefore, all mice were sacrificed 30 min after irradiation to determine γ-H2AX expression levels (Figure 3C, treatment scheme). Mice that received only irradiation (16 Gy) showed significantly elevated levels of γ-H2AX compared to control mice (Figure 3C). A significant decrease in γ-H2AX levels down to basal levels by a factor of 2.4, 1.7, and 2 was detected in the heart lysates of mice receiving CBD treatment 2 weeks prior to and after irradiation (Figure 3C). No elevation in γ-H2AX levels was seen in CBD-treated mice compared to control mice at 30 min. Pilot data (n = 2) show strongly elevated γ-H2AX levels (3.19-fold, 5-fold) 15 min after heart irradiation with 16 Gy, which could be reduced by a factor of 1.5 and 1.3 by 2-week pre-treatment with CBD (Appendix A.2). These findings suggest that treatment

with CBD prior to irradiation might reduce the occurrence of DNA double-strand damage in the irradiated tissue by supporting the repair of DNA double-strand breaks.

### CBD treatment starting 2 weeks before irradiation increases VCAM-1 on heart ECs

Although CBD treatment beginning 2 weeks prior to irradiation attenuates the upregulation of the inflammation markers MCAM and ICAM-1 after 2 and 10 weeks (Figure 2), a different expression pattern was observed for VCAM-1 (Figure 4). Mice receiving partial heart (80%) and lung (20%) irradiation with 16 Gy or partial heart irradiation (16 Gy) combined with daily i.p. injections of CBD (20 mg/kg body weight) for 4 weeks beginning 2 weeks prior to irradiation showed no significant upregulation in VCAM-1 on heart ECs compared to sham-treated controls 2 weeks after irradiation (Figure 4). This is consistent with previous findings that VCAM-1 upregulation in the heart manifests late after irradiation, with a significant increase only being observed 10 but not 5 weeks after irradiation with only 8 Gy [22]. At 10 weeks after irradiation, the expression of VCAM-1 in irradiated heart ECs was significantly upregulated, and this value increased even further when mice were treated for 4 weeks with CBD starting 2 weeks prior to irradiation (Figure 4).

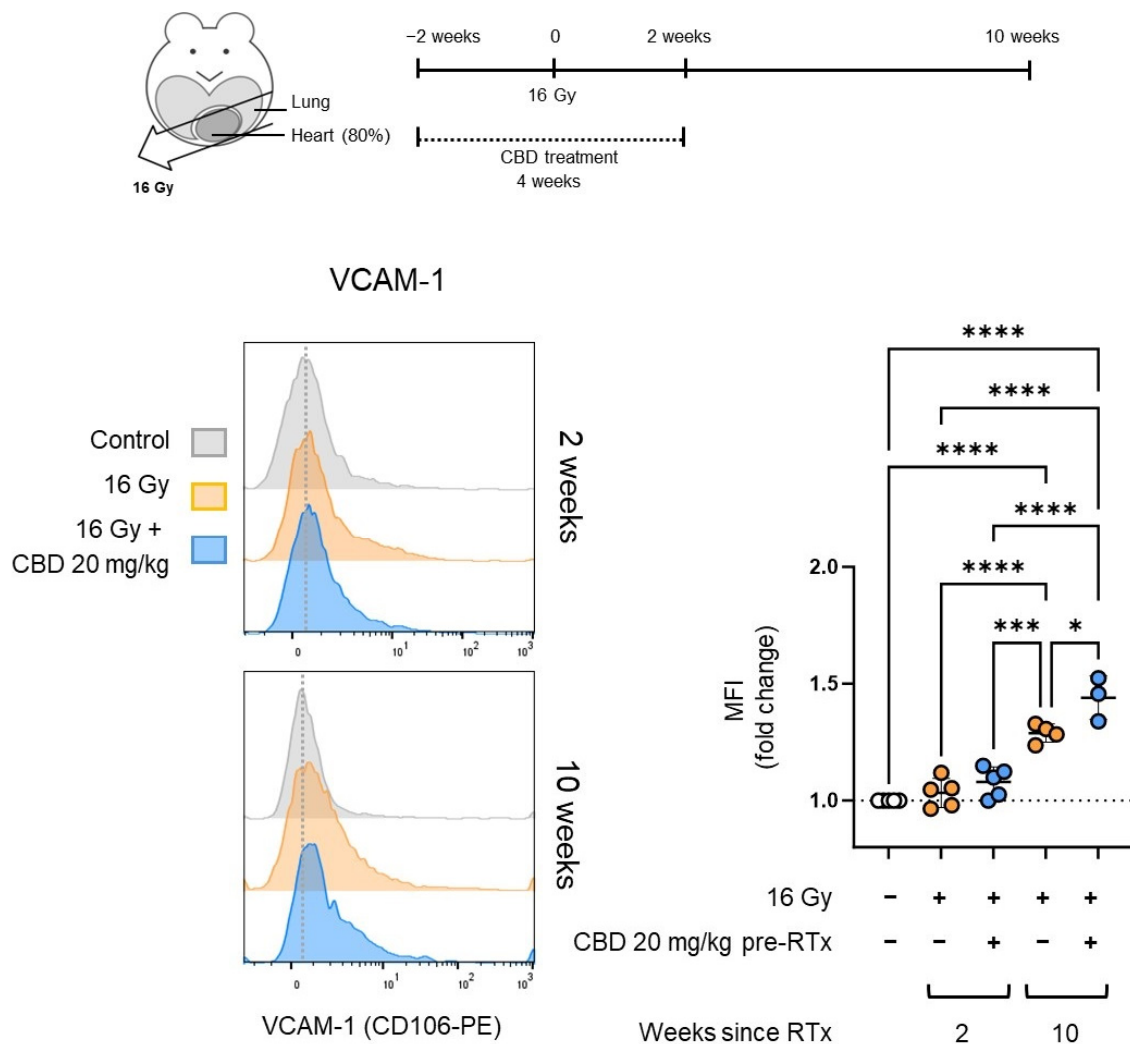


**Figure 4.** Representative fluorescence histograms of VCAM-1 expression and median signal intensity (MFI) on primary cardiac ECs ( $CD31^+/CD45^-$ ) of C57BL/6 mice 2 ( $n = 5$ ) and 10 ( $n = 3-4$ ) weeks after receiving 0 Gy sham irradiation (white), 16 Gy irradiation (orange), or 16 Gy irradiation with daily CBD treatment starting 2 weeks prior to irradiation (i.p., 20 mg/kg body weight for 4 weeks; blue); data represent mean values  $\pm$  SD of 4 mice ( $n = 3-5$ ); \*  $p < 0.05$ , \*\*\*  $p < 0.001$ , and \*\*\*\*  $p < 0.0001$ .

### **CBD treatment starting 2 weeks before irradiation reduces immune cell infiltration into the heart**

To investigate why VCAM-1 expression differs from that of other inflammatory markers, such as MCAM, ICAM-1, and ICAM-2, in response to CBD treatment, different mediators responsible for the induction of VCAM-1 expression were analyzed. Tumor necrosis factor alpha (TNF- $\alpha$ ) is a major inducer of VCAM-1 [31], which is produced mainly by macrophages [32]. Infiltration of leukocytes and macrophages into irradiated tissues like the heart occurs several weeks after irradiation [33] and shows a similar kinetic to the increase in the expression of VCAM-1 on heart ECs [22]. Therefore, we investigated the presence of immune cells, such as CD45<sup>+</sup> leukocytes (Figure 5A), in single cell suspensions derived from whole hearts of mice receiving sham irradiation (0 Gy), partial heart (80%) and lung (20%) irradiation with 16 Gy, or irradiation of the heart (16 Gy) combined with daily i.p. injections of CBD (20 mg/kg body weight) for 4 weeks beginning 2 weeks prior to irradiation. Mice were sacrificed 2 and 10 weeks after irradiation, and heart-derived single cell suspensions were assessed through flow cytometry (n = 3–5, Figure 5A). We further determined the presence of CD14<sup>+</sup> macrophages (Figure 5B) [34] in the same mouse groups 10 weeks after irradiation (n = 3–4) through Western blot analysis of whole heart lysates. We found that 2 weeks after irradiation, the proportion of infiltration of CD45<sup>+</sup> leukocytes remained unaltered in all treatment groups. However, 10 weeks after irradiation, the presence of leukocytes significantly increased in the hearts of mice receiving irradiation. CBD treatment prior to irradiation resulted in a significant reduction in immune cell infiltration of the heart (Figure 5A). Similarly to CD45<sup>+</sup> leukocytes, the percentage of infiltrating CD14<sup>+</sup> macrophages increased significantly 10 weeks after irradiation of the mouse heart, whereas pre-treatment with CBD significantly reduced the infiltration of CD14<sup>+</sup> macrophages into the heart (Figure 5B). These findings suggest that upregulated VCAM-1 expression is not directly related to the presence or absence of immune cells in the heart 10 weeks after irradiation. Nevertheless, as immune infiltration contributes greatly to the development of long-term heart conditions observed after irradiation [35], with macrophages likely being the main mediators in cardiac fibrosis [17,36], a reduction in the proportion of infiltrating macrophages by CBD can be considered a potentially beneficial anti-fibrotic effect.

### **CBD treatment starting 2 weeks before irradiation reduces the expression of early fibrosis markers in the heart**

Although VCAM-1 expression shows a stronger association with the development of cardiac pathologies like atherosclerosis [37] than ICAM-1 and other CAMs, the increased expression of VCAM-1 10 weeks after irradiation by CBD treatment is contrasted by the CBD-mediated attenuation of the expression levels of MCAM and ICAM-1, the attenuation of DNA double-strand breaks, decreased immune infiltration, and an increased cytoprotective and anti-oxidative heat shock response. To conclude whether the overall effect of CBD treatment is beneficial to the heart or not, we investigated the whole heart lysate of mice that received sham irradiation (0 Gy), irradiation of the heart (80%) with 16 Gy, or irradiation of the heart (16 Gy) combined with daily i.p. injections of CBD (20 mg/kg body weight) for 4 weeks beginning 2 weeks prior to irradiation and sacrificed 10 weeks after irradiation for signs of fibrosis using Western blot analysis (Figure 6, treatment scheme). Specifically, we investigated levels of Col3a1, the peptide component of collagen III, which accumulates in cardiac fibrosis [38] (Figure 6A), Fibronectin, a classic fibrosis marker essential for the attachment of collagen to the extracellular matrix, which may also function as a damage-associated molecular pattern (DAMP) [39] (Figure 6B), and Decorin, a protein that is commonly upregulated in fibrotic tissue that participates in collagen fibril formation and also functions as a pro-inflammatory DAMP molecule [40] (Figure 6C). Col3a1 and

Fibronectin levels followed a similar expression pattern, with significant upregulation 10 weeks after irradiation, but normalized to control levels when mice received CBD treatment beginning 2 weeks prior to irradiation (Figure 6A,B). Decorin levels were significantly increased compared to controls in both irradiated groups, with CBD pre-treatment significantly attenuating the irradiation-induced upregulation of Decorin compared to untreated irradiated mice (Figure 6C). Taken together, these findings suggest that there is an ongoing damage response with fibrotic characteristics in the heart 10 weeks after irradiation that is attenuated by CBD pre-treatment.

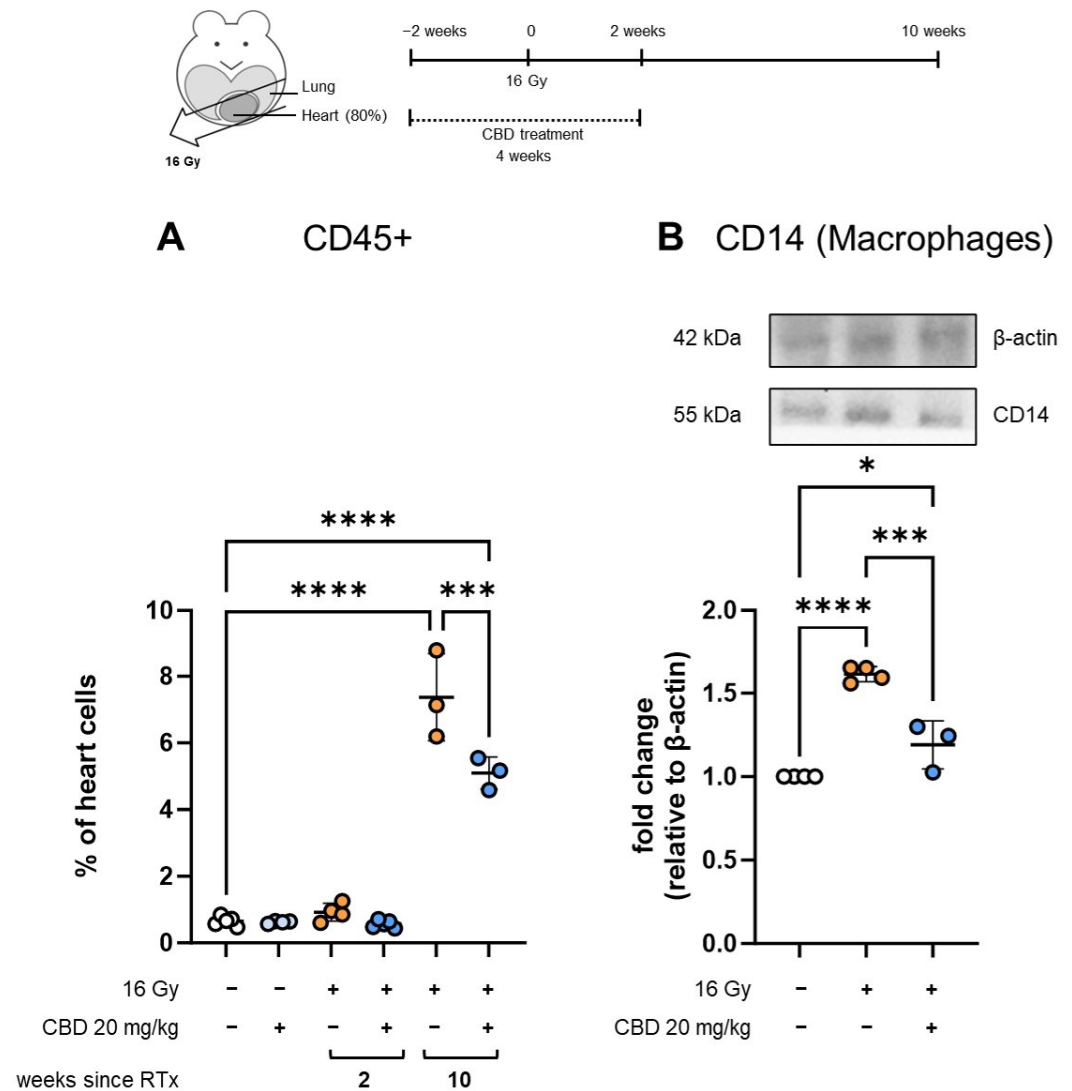


**Figure 5.** Percentage of CD45<sup>+</sup> leukocytes (A) and presence of CD14<sup>+</sup> macrophages (B) in single cell suspensions of whole heart tissues of C57BL/6 mice 2 (n = 5) and 10 (n = 3) weeks after receiving 0 Gy sham irradiation (white), daily CBD treatment starting 2 weeks prior to sham irradiation (i.p., 20 mg/kg body weight for 4 weeks; light blue), 16 Gy irradiation (orange), or 16 Gy irradiation with daily CBD treatment starting 2 weeks prior to irradiation (i.p., 20 mg/kg body weight for 4 weeks; blue); data represent mean values ± SD of 3–4 mice (n = 3–4); \* p < 0.05, \*\*\* p < 0.001, and \*\*\*\* p < 0.0001). Representative Western blot and mean protein levels relative to β-actin of CD14 in whole heart lysate of C57BL/6 mice (n = 3–4) 10 weeks after receiving sham irradiation (0 Gy, left lane, white symbol), 16 Gy irradiation (center lane, orange symbol), or 16 Gy irradiation with daily CBD treatment starting 2 weeks prior to irradiation (i.p., 20 mg/kg body weight; right lane, blue symbol); data represent mean values ± SD of 3 to 5 mice (n = 3–5); \* p < 0.05, \*\*\* p < 0.001, and \*\*\*\* p < 0.0001.

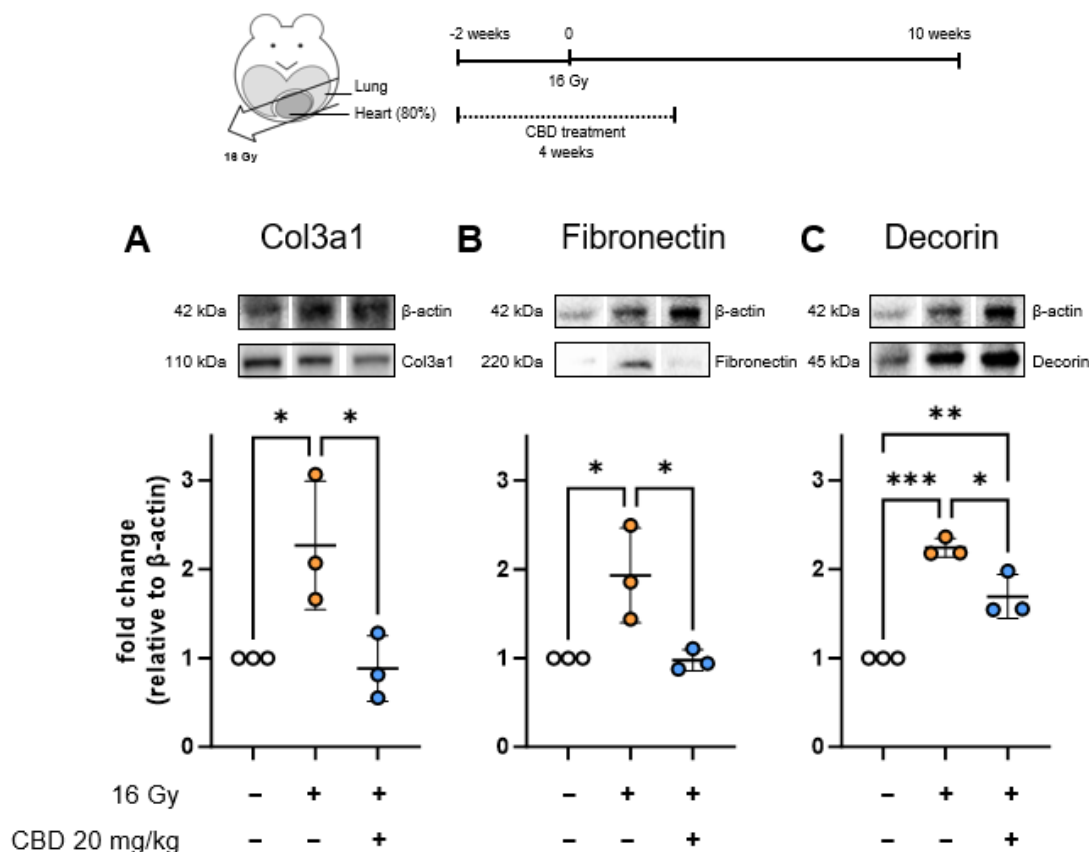


**Figure 6.** Fibrosis-associated protein levels in whole heart lysates of C57BL/6 mice; representative Western blot images of  $\beta$ -actin and (A) Col3a1, (B) Fibronectin, and (C) Decorin and average fold change of protein levels relative to  $\beta$ -actin and normalized to control of mice 10 weeks after 0 Gy sham irradiation (left band, white symbol), 16 Gy irradiation (center band, orange symbol), or 16 Gy irradiation with 4-week daily CBD treatment starting 2 weeks prior to irradiation (i.p., 20 mg/kg body weight; right band, blue symbol); data represent mean values  $\pm$  SD of 3 mice ( $n = 3$ ); \*  $p < 0.05$ , \*\*  $p < 0.01$ , \*\*\*  $p < 0.001$ .

#### 4. Discussion

In this study, we found that a 4-week treatment with 20 mg/kg of CBD beginning 2 weeks prior to irradiation (16 Gy) can attenuate the irradiation-induced upregulation of the inflammatory cell adhesion molecules ICAM-1, MCAM, and, potentially, ICAM-2 on cardiac ECs. However, CBD treatment of the same duration did not result in attenuation of these inflammation markers when treatment was started at the time of irradiation. This suggests that CBD exerts a radioprotective effect during irradiation, with the decreased inflammation being a result of reduced damage suffered by the cardiac ECs, rather than repairing radiation-induced damage. This hypothesis is further supported by the finding that CBD treatment beginning 2 weeks prior to irradiation results in a lower rate of irradiation-induced DNA double-strand breaks in cardiac cells, as indicated by  $\gamma$ -H2AX levels. This is an effect we previously described in ECs that had been pre-treated in vitro with CBD 24 h before irradiation and that also resulted in a reduced rate of EC apoptosis [41].

The proposed mediators of this effect are Hsp32/HO-1 and Hsp70, which we found to be significantly elevated in the cardiac tissue of mice that received daily CBD injections in addition to irradiation (16 Gy) but not in mice that received only irradiation. While Hsps are upregulated in response to cellular stressors, including irradiation-induced oxidative stress [42], they can also be induced by triggers that are not lethal or cytotoxic, such as a mild heat exposure [43]. Upregulated levels of Hsps have frequently been shown to exert

protection from severe stressors, and they have protective effects in cardiac conditions, such as ischemia [44,45] and cardiac dysfunction [19]. Hsp32/HO-1 and Hsp70 in particular have demonstrated an ability to adapt cells to oxidative stress [29], with Hsp70 also possibly acting as an inducer of Hsp32/HO-1 [46]. The antioxidative and cytoprotective effects of Hsp32/HO-1 [47] and Hsp70 are generally well-established [48,49]. The fact that Hsp induction may take 24 to 48 h to reach peak levels depending on circumstances [43,45] supports the notion that CBD treatment needs to be started with a sufficient leadup time to enable maximum levels of Hsps to be reached at the time of irradiation. However, a shorter leadup time than the 2 weeks used in this study might also suffice but was not tested in this study. The CBD-mediated induction of Hsp32/HO-1 in ECs has been described previously by others [28], as well as us [41]. In this study, we showed for the first time that in addition to Hsp32/HO-1, Hsp70 was also found to be upregulated after *in vivo* CBD treatment followed by irradiation. Our previous finding that ECs of cell line origin, as well as primary lung ECs that were pre-treated with CBD for 24 h, showed lower levels of ROS production upon irradiation, which correlated with increased levels of Hsp32/HO-1 [41] and Hsp70, provides insight into how CBD may be reducing irradiation-induced damage to the tissue.

CBD treatment starting 2 weeks prior to irradiation and concluding 2 weeks after irradiation also resulted in a reduced infiltration of immune cells, specifically CD14<sup>+</sup> macrophages, into the heart at 10 weeks. Although at 2 weeks there was not yet an increase in immune cells in any group despite there being a significant upregulation of some CAMs at this timepoint, our findings are nonetheless consistent with the trajectory of a continuous upregulation of the CAMs over multiple weeks seen in this and previous studies [22,50] and with immune infiltration also being detected at significant levels only after multiple weeks after irradiation [33]. It may also suggest the importance of VCAM-1 in the transmigration of immune cells across the endothelial barrier, as VCAM-1 is the only CAM that had not yet increased at 2 weeks. The indication that VCAM-1 and ICAM-1 cooperate and are both required for optimal leukocyte adhesion and transmigration [51,52] possibly explains why attenuation of ICAM-1 results in decreased leukocyte presence even in the absence of VCAM-1 attenuation. Blockades of either ICAM-1 or VCAM-1 have both resulted in significant decreases in leukocyte transmigration [53,54]. Due to the significant role the adherence and infiltration of immune cells into the vascular walls play in the development of the atherosclerosis and cardiomyopathy that can follow cardiac irradiation [35], the reduced levels of immune cells we detected 10 weeks after irradiation are a promising sign that CBD reduces or delays the progression of RIHD.

We also showed that 10 weeks after irradiation, levels of the fibrosis-associated proteins Fibronectin, Decorin, and the component of collagen III, Col3a1, in the heart tissue are reduced when mice received CBD pre-treatment starting 2 weeks before irradiation (16 Gy) compared to mice that received no treatment in addition to irradiation. This suggests that CBD may attenuate the development of cardiac fibrosis after irradiation. However, due to the slow development of fibrotic lesions [13], longer follow-up after irradiation should be targeted in future studies. Although cardiac fibrosis after irradiation develops continuously over time, the first signs of fibrosis have been found at latency periods similar to our treatment regimen (10 weeks after irradiation), such as the occurrence of systolic dysfunction in mice 3 months after 12–20 Gy irradiation [55], the appearance of fibrotic lesions characterized by collagen deposits, fibrin presence, and thickened fibrous membranes in rabbits starting 75 days after irradiation with 2000–4000 rad (20–40 Gy) [56], and the appearance of fibrotic lesions in C57BL/6 mice 8 weeks after 40–60 Gy irradiation (although significance was not reached until a later timepoint) [57].

Curiously, the expression of the inflammatory marker VCAM-1 does not follow the same pattern shared by MCAM, ICAM-1, and ICAM-2, which are upregulated more rapidly

than VACM-1 after irradiation. There is no significant upregulation of VCAM-1 2 weeks after irradiation, consistent with previous studies finding that VCAM-1 is upregulated later after irradiation [22]. Four weeks after irradiation, VCAM-1 is significantly upregulated but still at lower levels than the other CAMs, and CBD treatment starting at the time of irradiation can reduce VCAM-1 expression, contrary to the other studied CAMs, which did not benefit from this CBD treatment regimen. This finding might be due to the later onset (2-week difference) of VCAM-1 expression, which allows CBD to attenuate irradiation-induced VCAM-1 upregulation. Even more conflicting, we found that while at 10 weeks the other CAMs are attenuated by CBD treatment starting prior to irradiation, VCAM-1 levels are instead higher in the irradiated and CBD-treated mice than in the irradiated and untreated mice. Due to the similar timelines of significant macrophage infiltration [33] and VCAM-1 upregulation beginning to be detectable only multiple weeks after irradiation, we investigated if macrophage presence was associated with VCAM-1 levels in the irradiated groups. However, we could not find a compelling correlation between the increased expression of VCAM-1 in irradiated, CBD-treated mice and the presence of macrophages and CD45<sup>+</sup> immune cells. The detection of macrophages based on CD14 levels using Western blot analysis has some limitations, as other cells can also express CD14, albeit at much lower levels than macrophages [34]. Additionally, the fact that we did not distinguish between classically activated or alternatively activated macrophages allows for the possibility that the type of macrophage, rather than merely the amount, plays a role in VCAM-1 induction. While we are currently unable to give an explanation for the differing response of VCAM-1, overall, the results of this study indicate that the upregulation of VCAM-1 does not counter the predominantly beneficial effect of CBD.

The health of the heart and lungs is heavily interconnected, and damage to one organ can compound damage to the other through reciprocal effects [58]. Modifying irradiation planning to spare more of the heart may come at the cost of an increased dose to the lung, a radiosensitive organ with a dose rate limiting role in the clinical setting due to the serious and potentially fatal risks of irradiation-induced lung disease [4]. As a consequence, changing irradiation planning in favor of the heart may not increase overall patient health if it comes at the expense of the lung. In our model, the lung also received partial irradiation of 16 Gy to approximately 20% of the volume of the lungs. We previously showed that under these conditions, CBD treatment with 20 mg/kg body weight was also effective in attenuating signs of irradiation-induced inflammation in the lung, with inflammatory and angiogenic markers being mostly normalized to control levels by CBD at the investigated timepoints of 2 and 10 weeks after irradiation with 16 Gy [41]. Due to the apparent radioprotective effect of CBD on both the heart and lung tissue, CBD could alleviate concerns about the reciprocal effect in simultaneous irradiation delivered to the heart and lungs. With respect to other comorbidities of lung cancer patients with congestive heart failure (CHF) [59], such as obstructive pulmonary disease (COPD), peripheral vascular disease (PVD), cerebrovascular disease (CEVD), and renal diseases, CBD has been shown to reduce lung inflammation in a COPD mouse model [60], and, in humans, CBD has potential beneficial effects on PVD, CEVD, and CHF [61] due to its anti-inflammatory, anti-fibrotic, and vasorelaxation effects and endothelial protective effects. Moreover, CBD has shown no negative effects in patients with mild to severe renal impairment [62].

The strong upregulation of the stress response proteins Hsp32/HO-1 and Hsp70 by CBD may put into question whether this is induced by a potentially unsafe level of stress. However, CBD has been repeatedly shown to be well-tolerated in various clinical trials [20,63,64]. A dose of 20 mg/kg body weight showed no effect on body weight over an 11-week treatment period in one murine trial [19], and another murine trial with concentrations of 100 mg/kg body weight and a treatment regimen lasting 6 months

was also reported to be well-tolerated, although no organs beside the brain were investigated [65]. In a study specifically investigating hepatotoxicity in a murine model, CBD was administered daily for 10 days in doses between 61.5 mg/kg and 615 mg/kg, showing some degree of hepatotoxicity at all doses [66]. However, a minor risk of hepatotoxicity exists for many drugs, including ‘over the counter’ medication, and hepatotoxicity frequently occurs in anti-cancer drugs [67,68]. In the context of using CBD as a radioprotective agent, the risk of hepatotoxicity needs to be weighed against the risk of developing radiation-induced pathologies.

Future studies are required to elucidate CBD’s radioprotective mechanism of action in detail, especially considering that systemically administered CBD is likely to affect a variety of resident cardiac cells, like smooth muscle cells and ECs [69], as well as immune cells, such as macrophages [70], and potentially do so through differing mechanisms. While we investigated multiple molecular markers indicative of cardiac inflammation and the development of fibrosis, histological and functional evidence of these findings is not provided by our study. It may be prudent to explore these parameters next and monitor the development of inflammation and fibrosis after latency periods longer than 10 weeks, as irradiation-induced cardiac toxicity can persist for over a year in rodent models [50,71] and longer still in humans [6]. Another valuable issue to explore is whether other normal tissues that are commonly affected by radiotherapy-related toxicity may also benefit from CBD treatment. Finally, carrying out combined tumor and radiotherapy models will be necessary to confirm that CBD can protect normal tissue without interfering with the anti-tumor efficacy of radiotherapy.

## 5. Conclusions

Overall, the results of this study show that CBD treatment can improve multiple symptoms of irradiation-induced damage to the heart, with effects persisting even 8 weeks after the conclusion of CBD treatment. The attenuation of MCAM and ICAM-1 when the 4-week CBD treatment was started 2 weeks prior to irradiation but not when treatment was started only at the time of irradiation, as well as the CBD-mediated reduction in acute DNA damage, suggests that the CBD-mediated effects are, at least partially, protective, and require a treatment regimen beginning with sufficient leadup to irradiation. The elevated levels of the stress proteins Hsp32/HO-1 and Hsp70 through CBD treatment are likely mediators of these radioprotective effects. Lastly, the potentially unfavorable increase in VCAM-1 expression seen with CBD treatment appears to be outweighed by the favorable effect of CBD on the other investigated parameters, even though the reason for VCAM-1’s divergent response to CBD remains to be determined. In summary, CBD shows strong promise as a potential radioprotective agent to reduce normal tissue toxicity to the heart and improve patients’ long-term health after radiotherapy.

**Supplementary Materials:** The following supporting information can be downloaded at <https://www.mdpi.com/article/10.3390/radiation5020017/s1>, Table S1: Raw data of Figure 1; Table S2: Raw data of Figure 2; Table S3: Raw data of Figure 3; Table S4: Raw data of Figure 4; Table S5: Raw data of Figure 5; Table S6: Raw data of Figure 6; Table S7: Raw data of Appendix A.1; Figure S1: Annotated Western blot images.

**Author Contributions:** Conceptualization, G.M.; methodology, L.B., B.A., M.B., M.J. and K.H.; software, M.H.K.; validation, G.M., G.R. and A.G.P.; formal analysis, G.M. and L.B.; investigation, L.B. and B.A.; resources, G.M.; data curation, G.M. and L.B.; writing—original draft preparation, L.B.; writing—review and editing, G.M. and A.G.P.; visualization, L.B., K.H. and M.H.K.; supervision, G.M. and G.R.; project administration, G.M.; funding acquisition, G.M. All authors have read and agreed to the published version of the manuscript.

**Funding:** This research was funded by the German Federal Ministry of Education and Research (BMBF) under grant 02NUK064A and 02NUK064B.

**Institutional Review Board Statement:** Animal experiments were performed in compliance with the institutional guidelines of the Technische Universität München and approved by the Regierung Oberbayern (ROB-55.2-2532.Vet\_02-21-195, 22 October 2022, and ROB-55.2-2532.Vet\_02-23-53, 9 September 2023).

**Informed Consent Statement:** Not applicable.

**Data Availability Statement:** The original contributions presented in the study are included in the Supplementary Materials; further inquiries can be directed to the corresponding author.

**Acknowledgments:** The authors thank Anett Lange and Ali Bashiri Dezfouli for their technical assistance.

**Conflicts of Interest:** The authors declare no conflicts of interest.

## Abbreviations

CBD	Cannabidiol
CAM	Cell adhesion molecule
HO-1	Heme-oxygenase-1
Hsp	Heat shock protein
ICAM	Intercellular adhesion molecule
Ig	Immunoglobulin
mAb	Monoclonal antibody
MCAM	Melanoma cell adhesion molecule
PVDF	Polyvinylidene fluoride
RIHD	Radiation-induced heart disease
SARRP	Small Animal Radiation Research Platform
SD	Standard deviation
TNF- $\alpha$	Tumor necrosis factor alpha
VCAM-1	Vascular cell adhesion molecule 1

## Appendix A

### Appendix A.1

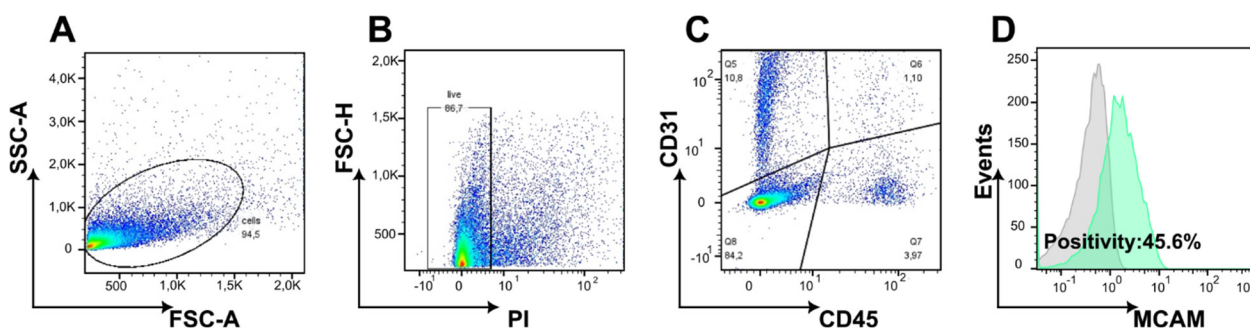


**Figure A1.** Gating strategy for the expression of MCAM (as an example) on CD31<sup>+</sup>/CD45<sup>-</sup> ECs through multicolor flow cytometry. Identification of the relevant cell population using a forward scatter area (FSC-A) vs. a side scatter area (SSC-A) dot plot (A), followed by the selection of viable cells through the exclusion of propidium iodide (PI)-positive (non-viable) cells (B). ECs were then gated based on CD31 positivity and CD45 negativity (CD31<sup>+</sup>/CD45<sup>-</sup>) (C). MCAM expression was evaluated on CD31<sup>+</sup>/CD45<sup>-</sup> ECs using an isotype-matched control antibody (gray histogram) and an MCAM-specific antibody (green histogram) (D).

## Appendix A.2

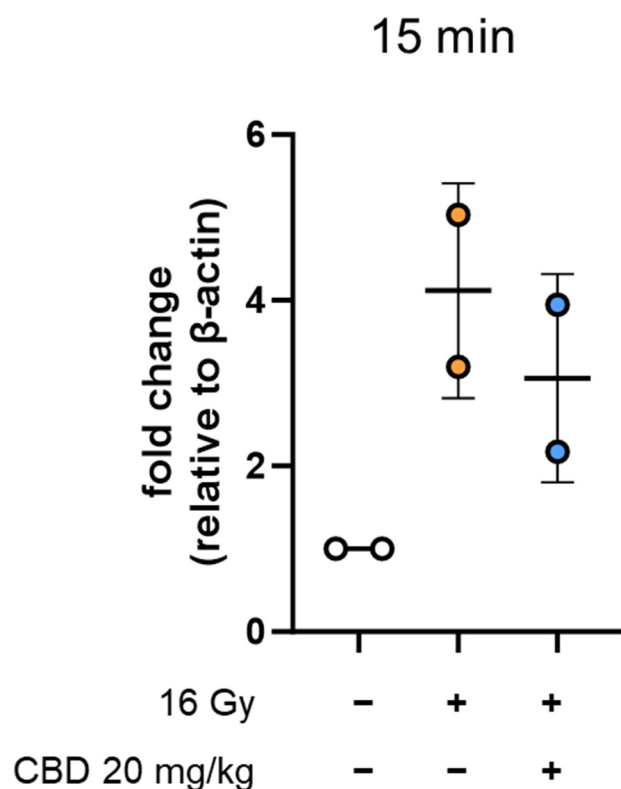


**Figure A2.** Western blot analysis of  $\gamma$ -H2AX protein levels relative to control of whole heart lysates derived from C57BL/6 mice 15 min after sham irradiation (0 Gy; white symbol), 16 Gy irradiation (orange symbol), or 16 Gy irradiation combined with daily CBD treatment starting 2 weeks prior to irradiation (i.p., 20 mg/kg body weight; blue symbol); data represent mean values  $\pm$  SD of 1 mouse (n = 1) with 2 technical replicates.

## References

- Baskar, R.; Dai, J.; Wenlong, N.; Yeo, R.; Yeoh, K.W. Biological response of cancer cells to radiation treatment. *Front. Mol. Biosci.* **2014**, *1*, 24. [[CrossRef](#)] [[PubMed](#)]
- Rakotomalala, A.; Escande, A.; Furlan, A.; Meignan, S.; Lartigau, E. Hypoxia in Solid Tumors: How Low Oxygenation Impacts the "Six Rs" of Radiotherapy. *Front. Endocrinol.* **2021**, *12*, 742215. [[CrossRef](#)]
- Baselet, B.; Sonveaux, P.; Baatout, S.; Aerts, A. Pathological effects of ionizing radiation: Endothelial activation and dysfunction. *Cell. Mol. Life Sci.* **2019**, *76*, 699–728. [[CrossRef](#)]
- Beach, T.A.; Groves, A.M.; Williams, J.P.; Finkelstein, J.N. Modeling radiation-induced lung injury: Lessons learned from whole thorax irradiation. *Int. J. Radiat. Biol.* **2020**, *96*, 129–144. [[CrossRef](#)] [[PubMed](#)]
- Zhu, W.; Zhang, X.; Yu, M.; Lin, B.; Yu, C. Radiation-induced liver injury and hepatocyte senescence. *Cell. Death Discov.* **2021**, *7*, 244. [[CrossRef](#)] [[PubMed](#)]
- Belzile-Dugas, E.; Eisenberg, M.J. Radiation-Induced Cardiovascular Disease: Review of an Underrecognized Pathology. *J. Am. Heart Assoc.* **2021**, *10*, e021686. [[CrossRef](#)]
- Darby, S.C.; Ewertz, M.; McGale, P.; Bennet, A.M.; Blom-Goldman, U.; Brønnum, D.; Correa, C.; Cutter, D.; Gagliardi, G.; Gigante, B.; et al. Risk of ischemic heart disease in women after radiotherapy for breast cancer. *N. Engl. J. Med.* **2013**, *368*, 987–998. [[CrossRef](#)]
- Drost, L.; Yee, C.; Lam, H.; Zhang, L.; Wronski, M.; McCann, C.; Lee, J.; Vesprini, D.; Leung, E.; Chow, E. A Systematic Review of Heart Dose in Breast Radiotherapy. *Clin. Breast Cancer* **2018**, *18*, e819–e824. [[CrossRef](#)]
- Wollschläger, D.; Karle, H.; Stockinger, M.; Bartkowiak, D.; Bührdel, S.; Merzenich, H.; Wiegel, T.; Blettner, M.; Schmidberger, H. Radiation dose distribution in functional heart regions from tangential breast cancer radiotherapy. *Radiother. Oncol.* **2016**, *119*, 65–70. [[CrossRef](#)]
- Azzam, E.I.; Jay-Gerin, J.P.; Pain, D. Ionizing radiation-induced metabolic oxidative stress and prolonged cell injury. *Cancer Lett.* **2012**, *327*, 48–60. [[CrossRef](#)]

11. Devarakonda, S.; Thorsell, A.; Hedenström, P.; Rezapour, A.; Heden, L.; Banerjee, S.; Johansson, M.E.; Birchenough, G.; Morén, A.T.; Gustavsson, K.; et al. Low-grade intestinal inflammation two decades after pelvic radiotherapy. *EBioMedicine* **2023**, *94*, 104691. [[CrossRef](#)] [[PubMed](#)]
12. Schett, G.; Neurath, M.F. Resolution of chronic inflammatory disease: Universal and tissue-specific concepts. *Nat. Commun.* **2018**, *9*, 3261. [[CrossRef](#)] [[PubMed](#)]
13. Moisaner, M.; Skyttä, T.; Kivistö, S.; Huhtala, H.; Nikus, K.; Virtanen, V.; Kellokumpu-Lehtinen, P.L.; Raatikainen, P.; Tuohinen, S. Radiotherapy-induced diffuse myocardial fibrosis in early-stage breast cancer patients—Multimodality imaging study with six-year follow-up. *Radiat. Oncol.* **2023**, *18*, 124. [[CrossRef](#)] [[PubMed](#)]
14. Darby, S.C.; Cutter, D.J.; Boerma, M.; Constine, L.S.; Fajardo, L.F.; Kodama, K.; Mabuchi, K.; Marks, L.B.; Mettler, F.A.; Pierce, L.J.; et al. Radiation-related heart disease: Current knowledge and future prospects. *Int. J. Radiat. Oncol. Biol. Phys.* **2010**, *76*, 656–665. [[CrossRef](#)] [[PubMed](#)]
15. Schultz-Hector, S.; Trott, K.R. Radiation-induced cardiovascular diseases: Is the epidemiologic evidence compatible with the radiobiologic data? *Int. J. Radiat. Oncol. Biol. Phys.* **2007**, *67*, 10–18. [[CrossRef](#)]
16. Zhang, Z.; Liu, X.; Chen, D.; Yu, J. Radiotherapy combined with immunotherapy: The dawn of cancer treatment. *Signal Transduct. Target Ther.* **2022**, *7*, 258. [[CrossRef](#)]
17. Atalay, S.; Jarocka-Karpowicz, I.; Skrzydlewska, E. Antioxidative and Anti-Inflammatory Properties of Cannabidiol. *Antioxidants* **2019**, *9*, 21. [[CrossRef](#)]
18. Hinz, B.; Ramer, R. Cannabinoids as anticancer drugs: Current status of preclinical research. *Br. J. Cancer* **2022**, *127*, 1–13. [[CrossRef](#)]
19. Rajesh, M.; Mukhopadhyay, P.; Bátkai, S.; Patel, V.; Saito, K.; Matsumoto, S.; Kashiwaya, Y.; Horváth, B.; Mukhopadhyay, B.; Becker, L.; et al. Cannabidiol attenuates cardiac dysfunction, oxidative stress, fibrosis, and inflammatory and cell death signaling pathways in diabetic cardiomyopathy. *J. Am. Coll. Cardiol.* **2010**, *56*, 2115–2125. [[CrossRef](#)]
20. Iffland, K.; Grotenhermen, F. An Update on Safety and Side Effects of Cannabidiol: A Review of Clinical Data and Relevant Animal Studies. *Cannabis Cannabinoid Res.* **2017**, *2*, 139–154. [[CrossRef](#)]
21. Sievert, W.; Stangl, S.; Steiger, K.; Multhoff, G. Improved Overall Survival of Mice by Reducing Lung Side Effects After High-Precision Heart Irradiation Using a Small Animal Radiation Research Platform. *Int. J. Radiat. Oncol. Biol. Phys.* **2018**, *101*, 671–679. [[CrossRef](#)] [[PubMed](#)]
22. Sievert, W.; Trott, K.R.; Azimzadeh, O.; Tapio, S.; Zitzelsberger, H.; Multhoff, G. Late proliferating and inflammatory effects on murine microvascular heart and lung endothelial cells after irradiation. *Radiother. Oncol.* **2015**, *117*, 376–381. [[CrossRef](#)]
23. Bardin, N.; Blot-Chabaud, M.; Despoix, N.; Kebir, A.; Harhour, K.; Arsanto, J.P.; Espinosa, L.; Perrin, P.; Robert, S.; Vely, F.; et al. CD146 and its soluble form regulate monocyte transendothelial migration. *Arterioscler. Thromb. Vasc. Biol.* **2009**, *29*, 746–753. [[CrossRef](#)] [[PubMed](#)]
24. Halai, K.; Whiteford, J.; Ma, B.; Nourshargh, S.; Woodfin, A. ICAM-2 facilitates luminal interactions between neutrophils and endothelial cells in vivo. *J. Cell. Sci.* **2014**, *127 Pt 3*, 620–629.
25. Muller, W.A. How endothelial cells regulate transmigration of leukocytes in the inflammatory response. *Am. J. Pathol.* **2014**, *184*, 886–896. [[CrossRef](#)]
26. Anil, S.M.; Peeri, H.; Koltai, H. Medical Cannabis Activity Against Inflammation: Active Compounds and Modes of Action. *Front. Pharmacol.* **2022**, *13*, 908198. [[CrossRef](#)]
27. Pereira, S.R.; Hackett, B.; O'Driscoll, D.N.; Sun, M.C.; Downer, E.J. Cannabidiol modulation of oxidative stress and signalling. *Neuronal. Signal.* **2021**, *5*, NS20200080. [[CrossRef](#)] [[PubMed](#)]
28. Böckmann, S.; Hinz, B. Cannabidiol Promotes Endothelial Cell Survival by Heme Oxygenase-1-Mediated Autophagy. *Cells* **2020**, *9*, 1703. [[CrossRef](#)]
29. Khomenko, I.P.; Bakhtina, L.Y.; Zelenina, O.M.; Kruglov, S.V.; Manukhina, E.B.; Bayda, L.A.; Malyshev, I.Y. Role of heat shock proteins HSP70 and HSP32 in the protective effect of adaptation of cultured HT22 hippocampal cells to oxidative stress. *Bull. Exp. Biol. Med.* **2007**, *144*, 174–177. [[CrossRef](#)]
30. Rogakou, E.P.; Pilch, D.R.; Orr, A.H.; Ivanova, V.S.; Bonner, W.M. DNA double-stranded breaks induce histone H2AX phosphorylation on serine 139. *J. Biol. Chem.* **1998**, *273*, 5858–5868. [[CrossRef](#)]
31. Min, J.K.; Kim, Y.M.; Kim, S.W.; Kwon, M.C.; Kong, Y.Y.; Hwang, I.K.; Won, M.H.; Rho, J.; Kwon, Y.G. TNF-related activation-induced cytokine enhances leukocyte adhesiveness: Induction of ICAM-1 and VCAM-1 via TNF receptor-associated factor and protein kinase C-dependent NF-kappaB activation in endothelial cells. *J. Immunol.* **2005**, *175*, 531–540. [[CrossRef](#)] [[PubMed](#)]
32. Idriss, H.T.; Naismith, J.H. TNF alpha and the TNF receptor superfamily: Structure-function relationship(s). *Microsc. Res. Tech.* **2000**, *50*, 184–195. [[CrossRef](#)] [[PubMed](#)]
33. Cao, C.; Wu, R.; Wang, S.; Zhuang, L.; Chen, P.; Li, S.; Zhu, Q.; Li, H.; Lin, Y.; Li, M.; et al. Elucidating the changes in the heterogeneity and function of radiation-induced cardiac macrophages using single-cell RNA sequencing. *Front. Immunol.* **2024**, *15*, 1363278. [[CrossRef](#)]

34. Na, K.; Oh, B.C.; Jung, Y. Multifaceted role of CD14 in innate immunity and tissue homeostasis. *Cytokine Growth Factor Rev.* **2023**, *74*, 100–107. [[CrossRef](#)]
35. Wang, H.; Wei, J.; Zheng, Q.; Meng, L.; Xin, Y.; Yin, X.; Jiang, X. Radiation-induced heart disease: A review of classification, mechanism and prevention. *Int. J. Biol. Sci.* **2019**, *15*, 2128–2138. [[CrossRef](#)] [[PubMed](#)]
36. Hulsmans, M.; Sager, H.B.; Roh, J.D.; Valero-Muñoz, M.; Houstis, N.E.; Iwamoto, Y.; Sun, Y.; Wilson, R.M.; Wojtkiewicz, G.; Tricot, B.; et al. Cardiac macrophages promote diastolic dysfunction. *J. Exp. Med.* **2018**, *215*, 423–440. [[CrossRef](#)]
37. Cybulsky, M.I.; Iiyama, K.; Li, H.; Zhu, S.; Chen, M.; Iiyama, M.; Davis, V.; Gutierrez-Ramos, J.C.; Connelly, P.W.; Milstone, D.S. A major role for VCAM-1, but not ICAM-1, in early atherosclerosis. *J. Clin. Investig.* **2001**, *107*, 1255–1262. [[CrossRef](#)]
38. Li, L.; Zhao, Q.; Kong, W. Extracellular matrix remodeling and cardiac fibrosis. *Matrix Biol.* **2018**, *68–69*, 490–506. [[CrossRef](#)]
39. Meagher, P.B.; Lee, X.A.; Lee, J.; Visram, A.; Friedberg, M.K.; Connelly, K.A. Cardiac Fibrosis: Key Role of Integrins in Cardiac Homeostasis and Remodeling. *Cells* **2021**, *10*, 770. [[CrossRef](#)]
40. Dong, Y.; Zhong, J.; Dong, L. The Role of Decorin in Autoimmune and Inflammatory Diseases. *J. Immunol. Res.* **2022**, *2022*, 1283383. [[CrossRef](#)]
41. Bauer, L.; Alkotub, B.; Ballmann, M.; Hasanzadeh Kafshgari, M.; Rammes, G.; Multhoff, G. Cannabidiol (CBD) Protects Lung Endothelial Cells from Irradiation-Induced Oxidative Stress and Inflammation In Vitro and In Vivo. *Cancers* **2024**, *16*, 3589. [[CrossRef](#)] [[PubMed](#)]
42. Szyller, J.; Bil-Lula, I. Heat Shock Proteins in Oxidative Stress and Ischemia/Reperfusion Injury and Benefits from Physical Exercises: A Review to the Current Knowledge. *Oxid. Med. Cell. Longev.* **2021**, *2021*, 6678457. [[CrossRef](#)] [[PubMed](#)]
43. Moloney, T.C.; Hoban, D.B.; Barry, F.P.; Howard, L.; Dowd, E. Kinetics of thermally induced heat shock protein 27 and 70 expression by bone marrow-derived mesenchymal stem cells. *Protein Sci.* **2012**, *21*, 904–909. [[CrossRef](#)] [[PubMed](#)]
44. Issan, Y.; Kornowski, R.; Aravot, D.; Shainberg, A.; Laniado-Schwartzman, M.; Sodhi, K.; Abraham, N.G.; Hochhauser, E. Heme oxygenase-1 induction improves cardiac function following myocardial ischemia by reducing oxidative stress. *PLoS ONE* **2014**, *9*, e92246. [[CrossRef](#)]
45. Amrani, M.; Corbett, J.; Boateng, S.Y.; Dunn, M.J.; Yacoub, M.H. Yacoub, Kinetics of induction and protective effect of heat-shock proteins after cardioplegic arrest. *Ann. Thorac. Surg.* **1996**, *61*, 1407–1411. [[CrossRef](#)]
46. Deng, B.; He, X.; Wang, Z.; Kang, J.; Zhang, G.; Li, L.; Kang, X. HSP70 protects PC12 cells against TBHP-induced apoptosis and oxidative stress by activating the Nrf2/HO-1 signaling pathway. *In Vitro Cell. Dev. Biol. Anim.* **2024**, *60*, 868–878. [[CrossRef](#)]
47. Ryter, S.W. Heme Oxygenase-1: An Anti-Inflammatory Effector in Cardiovascular, Lung, and Related Metabolic Disorders. *Antioxidants* **2022**, *11*, 555. [[CrossRef](#)]
48. Bidmon-Fliegenschnee, B.; Lederhuber, H.C.; Csaicsich, D.; Pichler, J.; Herzog, R.; Memaran-Dadgar, N.; Huber, W.D.; Aufrecht, C.; Kratochwill, K. Overexpression of Hsp70 confers cytoprotection during gliadin exposure in Caco-2 cells. *Pediatr. Res.* **2015**, *78*, 358–364. [[CrossRef](#)]
49. Mazzei, L.; Docherty, N.G.; Manucha, W. Mediators and mechanisms of heat shock protein 70 based cytoprotection in obstructive nephropathy. *Cell Stress Chaperones* **2015**, *20*, 893–906. [[CrossRef](#)]
50. Wittmann, A.; Bartels, A.; Alkotub, B.; Bauer, L.; Kafshgari, M.H.; Multhoff, G. Chronic inflammatory effects of in vivo irradiation of the murine heart on endothelial cells mimic mechanisms involved in atherosclerosis. *Strahlenther. Onkol.* **2023**, *199*, 1214–1224. [[CrossRef](#)]
51. Van Buul, J.D.; Van Rijssel, J.; Van Alphen, F.P.; van Stalborch, A.M.; Mul, E.P.; Hordijk, P.L.I. ICAM-1 clustering on endothelial cells recruits VCAM-1. *J. Biomed. Biotechnol.* **2010**, *2010*, 120328. [[CrossRef](#)] [[PubMed](#)]
52. Muller, W.A. Mechanisms of leukocyte transendothelial migration. *Annu. Rev. Pathol.* **2011**, *6*, 323–344. [[CrossRef](#)]
53. Sumagin, R.I.H. Sarelius, Intercellular adhesion molecule-1 enrichment near tricellular endothelial junctions is preferentially associated with leukocyte transmigration and signals for reorganization of these junctions to accommodate leukocyte passage. *J. Immunol.* **2010**, *184*, 5242–5252. [[CrossRef](#)] [[PubMed](#)]
54. Pickett, J.R.; Wu, Y.; Zacchi, L.F.; Ta, H.T. Targeting endothelial vascular cell adhesion molecule-1 in atherosclerosis: Drug discovery and development of vascular cell adhesion molecule-1-directed novel therapeutics. *Cardiovasc. Res.* **2023**, *119*, 2278–2293. [[CrossRef](#)] [[PubMed](#)]
55. Shamseddine, A.; Patel, S.H.; Chavez, V.; Moore, Z.R.; Adnan, M.; Di Bona, M.; Li, J.; Dang, C.T.; Ramanathan, L.V.; Oeffinger, K.C.; et al. Innate immune signaling drives late cardiac toxicity following DNA-damaging cancer therapies. *J. Exp. Med.* **2023**, *220*, e20220809. [[CrossRef](#)]
56. Fajardo, L.F.; Stewart, J.R. Experimental radiation-induced heart disease. I. Light microscopic studies. *Am. J. Pathol.* **1970**, *59*, 299–316.
57. Dreyfuss, A.D.; Goia, D.; Shoniyozov, K.; Shewale, S.V.; Velalopoulou, A.; Mazzoni, S.; Avgousti, H.; Metzler, S.D.; Bravo, P.E.; Feigenberg, S.J.; et al. A Novel Mouse Model of Radiation-Induced Cardiac Injury Reveals Biological and Radiological Biomarkers of Cardiac Dysfunction with Potential Clinical Relevance. *Clin. Cancer Res.* **2021**, *27*, 2266–2276. [[CrossRef](#)]

58. Ghobadi, G.; Van Der Veen, S.; Bartelds, B.; De Boer, R.A.; Dickinson, M.G.; De Jong, J.R.; Faber, H. Physiological interaction of heart and lung in thoracic irradiation. *Int. J. Radiat. Oncol. Biol. Phys.* **2012**, *84*, e639–e646. [[CrossRef](#)]
59. Hernandez, D.; Cheng, C.Y.; Hernandez-Villafuerte, K.; Schlander, M. Survival and comorbidities in lung cancer patients: Evidence from administrative claims data in Germany. *Oncol. Res.* **2022**, *30*, 173–185. [[CrossRef](#)]
60. Ribeiro, A.; Almeida, V.I.; Costola-de-Souza, C.; Ferraz-de-Paula, V.; Pinheiro, M.L.; Vitoretti, L.B.; Gimenes-Junior, J.A.; Akamine, A.T.; Crippa, J.A.; Tavares-de-Lima, W.; et al. Cannabidiol improves lung function and inflammation in mice submitted to LPS-induced acute lung injury. *Immunopharmacol. Immunotoxicol.* **2015**, *37*, 35–41. [[CrossRef](#)]
61. Garza-Cervantes, J.A.; Ramos-González, M.; Lozano, O.; Jerjes-Sánchez, C.; García-Rivas, G. Therapeutic Applications of Cannabinoids in Cardiomyopathy and Heart Failure. *Oxid. Med. Cell. Longev.* **2020**, *2020*, 4587024. [[CrossRef](#)]
62. Tayo, B.; Taylor, L.; Sahebkar, F.; Morrison, G. A Phase I, Open-Label, Parallel-Group, Single-Dose Trial of the Pharmacokinetics, Safety, and Tolerability of Cannabidiol in Subjects with Mild to Severe Renal Impairment. *Clin. Pharmacokinet.* **2020**, *59*, 747–755. [[CrossRef](#)]
63. Dahlgren, M.K.; Lambros, A.M.; Smith, R.T.; Sagar, K.A.; El-Abboud, C.; Gruber, S.A. Clinical and cognitive improvement following full-spectrum, high-cannabidiol treatment for anxiety: Open-label data from a two-stage, phase 2 clinical trial. *Commun. Med.* **2022**, *2*, 139. [[CrossRef](#)]
64. Tang, Y.; Tonkovich, K.L.; Rudisill, T.M. The Effectiveness and Safety of Cannabidiol in Non-seizure-related Indications: A Systematic Review of Published Randomized Clinical Trials. *Pharmaceut. Med.* **2022**, *36*, 353–385. [[CrossRef](#)]
65. Dearborn, J.T.; Nelvagal, H.R.; Rensing, N.R.; Takahashi, K.; Hughes, S.M.; Wishart, T.M.; Cooper, J.D.; Wong, M.; Sands, M.S. Effects of chronic cannabidiol in a mouse model of naturally occurring neuroinflammation, neurodegeneration, and spontaneous seizures. *Sci. Rep.* **2022**, *12*, 11286. [[CrossRef](#)] [[PubMed](#)]
66. Ewing, L.E.; Skinner, C.M.; Quick, C.M.; Kennon-McGill, S.; McGill, M.R.; Walker, L.A.; ElSohly, M.A.; Gurley, B.J.; Koturbash, I. Hepatotoxicity of a Cannabidiol-Rich Cannabis Extract in the Mouse Model. *Molecules* **2019**, *24*, 1694. [[CrossRef](#)]
67. Suzuki, A.; Andrade, R.J.; Bjornsson, E.; Lucena, M.I.; Lee, W.M.; Yuen, N.A.; Hunt, C.M.; Freston, J.W. Freston, Drugs associated with hepatotoxicity and their reporting frequency of liver adverse events in Vigibase: Unified list based on international collaborative work. *Drug Saf.* **2010**, *33*, 503–522. [[CrossRef](#)] [[PubMed](#)]
68. Vincenzi, B.; Armento, G.; Spalato Ceruso, M.; Catania, G.; Leakos, M.; Santini, D.; Minotti, G.; Tonini, G. Drug-induced hepatotoxicity in cancer patients—implication for treatment. *Expert Opin. Drug Saf.* **2016**, *15*, 1219–1238. [[CrossRef](#)] [[PubMed](#)]
69. Teichmann, E.; Blessing, E.; Hinz, B. Non-Psychoactive Phytocannabinoids Inhibit Inflammation-Related Changes of Human Coronary Artery Smooth Muscle and Endothelial Cells. *Cells* **2023**, *12*, 2389. [[CrossRef](#)]
70. Frodella, C.M.; Liu, L.; Tan, W.; Pruett, S.B.; Kaplan, B.L. The mechanism by which cannabidiol (CBD) suppresses TNF-alpha secretion involves inappropriate localization of TNF-alpha converting enzyme (TACE). *Cell. Immunol.* **2024**, *397–398*, 104812. [[CrossRef](#)]
71. Walls, G.M.; O’Kane, R.; Ghita, M.; Kuburas, R.; McGarry, C.K.; Cole, A.J.; Jain, S.; Butterworth, K.T. Butterworth, Murine models of radiation cardiotoxicity: A systematic review and recommendations for future studies. *Radiother. Oncol.* **2022**, *173*, 19–31. [[CrossRef](#)] [[PubMed](#)]

**Disclaimer/Publisher’s Note:** The statements, opinions and data contained in all publications are solely those of the individual author(s) and contributor(s) and not of MDPI and/or the editor(s). MDPI and/or the editor(s) disclaim responsibility for any injury to people or property resulting from any ideas, methods, instructions or products referred to in the content.